AN APPROACH TO SUB-PIXEL SPATIAL RESOLUTION IN ROOM TEMPERATURE X-RAY DETECTOR ARRAYS WITH GOOD ENERGY RESOLUTION

W.K. WARBURTON
X-ray Instrumentation Associates (XIA), 2513 Charleston Road STE 207
Mountain View, CA 94043-1607, USA.

ABSTRACT

In this paper we examine a recently proposed concept for obtaining sub-pixel spatial resolution in compound semiconductors where hole transport properties are relatively poor. [1] This approach uses weighted sums and differences of local pixel signals to extract both accurate x-ray energy estimates and interpolate location at the sub-pixel level. A simple analysis, including noise estimates, suggests the possibility of obtaining locations at the 50-100 micron level using 1-2 mm wide stripe electrodes while obtaining 1-2% energy resolution for x-rays up to 100 keV. Following this examination, we will present the most recent experimental results from our program to develop electronics to implement this scheme.

INTRODUCTION:

Considerable interest has developed in recent years in producing imaging x-ray or gamma-ray detectors which operate at or near room temperature. Proposed applications include medical imaging, industrial inspection, astronomical imaging and nuclear monitoring. Some of these applications would also benefit from energy resolution: for example to reject Compton scatter in medical imaging or to image at different energies to locate specific isotopes in nuclear waste disposal applications.

Approaches to this problem to date have been to create either pixelated or striped detectors (See Refs. [2-4] for typical examples) and employ them in a binary mode where a pixel is either hit or not. Since the pixel is then the fundamental resolution unit in these detectors, large numbers of pixels or stripes are required to obtain good spatial resolution. This leads to two problems: first a large number of processing circuits are required; and, second, resolution rapidly becomes limited by the dimensions of the drifting charge clouds within the detectors. [5] The approach proposed here attempts to overcome these problems by monitoring the induced charge signals developed on neighboring sets of electrodes and using the temporal behavior of these signals both to interpolate interaction locations within the pixel dimension and also to produce a good estimate of the absorbed photon's energy in the presence of carrier losses due to hole trapping.

THE 1-D DETECTOR MODEL

To simplify the explanation, we will restrict the discussion to a 1-D (striped) detector. The second dimension could be found either with a crossed set of stripes or through the use of large pixels. The detector geometry is shown in Figure 1, where each stripe is connected to a charge sensitive amplifier. In a "typical" case the material would be D = 5 mm thick CZT with w = 1 mm wide stripes. A gamma-ray is absorbed at height z above and at location (x,y) with respect to one corner of pixel i. An external voltage V creates electric field E within the detector volume.

The charge induced on a differential electrode area may be found classically by the method of image charges, provided one realizes that, since there are two conductive electrode planes in the problem, a charge q at (x,y,z) creates an infinite series of pairs (index k) of image charges at mirror image locations $+z_k$ and $-z_k$ outside the detector. Integrating over pixel dimensions (x_n, x_p, y_n,y_p) gives Equation 1 for the

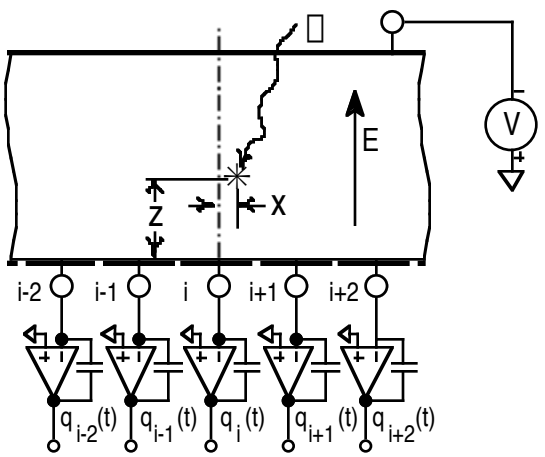

Fig. 1: Detector geometry near stripe electrode i.

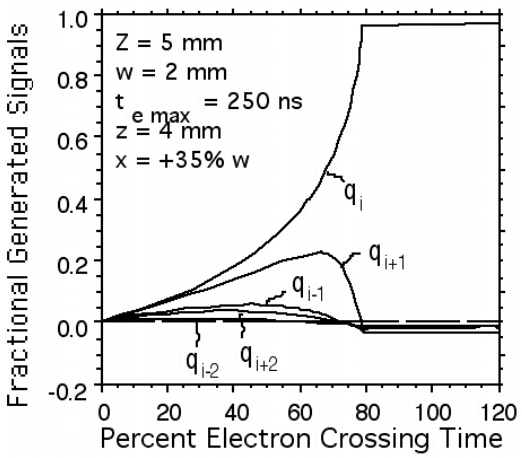

Fig. 2: Charge signals on pixels i-2 to i+2.

charge induced by image pair k, where the fences represent the 4 signed terms from the 4 limits of integration.

$$Q_{ijk} = \frac{q\,z}{2\pi}\int_{x_{in}}^{x_{ip}} dx \int_{y_{jn}}^{y_{jp}} \frac{dy}{(x^2+y^2+z_k^2)^{3/2}} = \frac{q}{4\pi}\left\| \sin^{-1}\left(\frac{x_{i\pm}^2(y_{j\pm}^2-z_k^2) - z_k^2(y_{j\pm}^2+z_k^2)}{x_{i\pm}^2(y_{j\pm}^2+z_k^2) + z_k^2(y_{j\pm}^2+z_k^2)}\right)\right\|_{x_n}^{x_p}\Bigg|_{y_n}^{y_p} \qquad (1)$$

Figure 2 shows the time evolution of the signals from 5 neighboring electrodes when D = 5 mm, V = 1000 V, w = 2 mm, z = 4 mm, and x = 0.85w (i.e. 15% of the way from the i+1 pixel edge) and there is no hole trapping.. Total electron transit time is 0.25 μs. As expected, only the hit electrode has any net charge after the end of the collection process. (The values are not yet precisely unity or zero yet because the holes are still moving.) The basis of our approach may be seen by comparing the signals on pixels i-1 and i+1. Since the interaction point is much closer to the latter, its signal is much larger. This difference may be used to determine x. Further, since only hole signal appears on pixels i-1 and i+1 just after electron collection, these values may be used to correct the signal on pixel i for hole effects.

We therefore create the following linear combinations of signals:

$$\text{Energy:} \quad E_i = Q_i - K_e\,(Q_{i-1} + Q_{i+1}) \qquad (2a)$$

$$\text{Location:} \quad L_i = Q_{i+1} - Q_{i-1} \qquad (2b)$$

$$\text{Timing:} \quad T_i = Q_{i-1} + Q_i + Q_{i+1} \qquad (2c)$$

$$\text{Slope:} \quad S_i = dE_i / dt; \qquad (2d)$$

The time evolution of these signals for the case of Fig. 2 is shown in Fig. 3 for a value of K_e of about 0.8. The energy signal E_i now comes very close to 1 and the slope signal S_i has a clear edge which can be used for transit timing.

DETERMINING LATERAL LOCATION

Figure 4 shows modeled L_i signals for a case similar to Fig. 2, except that z is 3 mm and the value of x is varied from 5% to 95% of the pixel width w. As expected from the definition of L_i, there is no signal when x = 0.5 (50%). We can then consider using L_i peak values (shown by dots) to determine x values.

An examination of the behavior of L_i as a function of z, as in Figure 5, shows that the L_i peak value is insufficient to determine x since this value depends upon the residual hole term remaining after electron collection, which term is sensitive to z. In

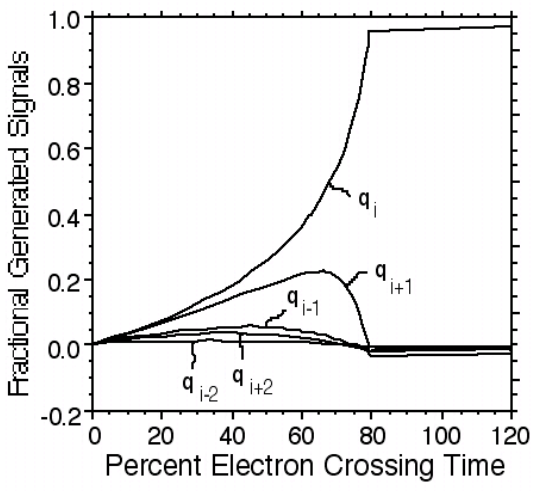

Fig. 3: Composite signals E_i, L_i, T_i, and S_i from Fig. 2.

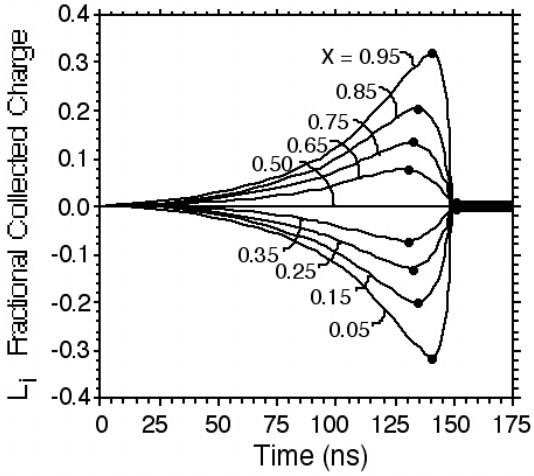

Fig. 4: L_i traces for a set of x position values.

fact, what is desired is the difference between the peak value and the value immediately after electron collection (i.e. the difference between pairs of dots in the Figure.). This difference can be shown to be quite z insensitive. [1]

Because of the difficulty in capturing and differencing these values, we have instead proposed [1] filtering the L_i signals with a trapezoidal shaping filter. Figure 6 shows the results of filtering curves like those of Figure 4 (expect w = 1 mm) with a filter having a 25 ns peaking time and a 25 ns flattop. The positive going peaks are now a good measure of x which is also z insensitive. These values are plotted in Figure 7 and show a fairly linear response as a function of x. The maximum deviations from linearity over the 5 - 95% x range are of order only 50 μm. Thus this approach offers considerable promise as a means of achieving spatial resolutions at the 50 to 100 μm scale using pixels with millimeter scale dimensions.

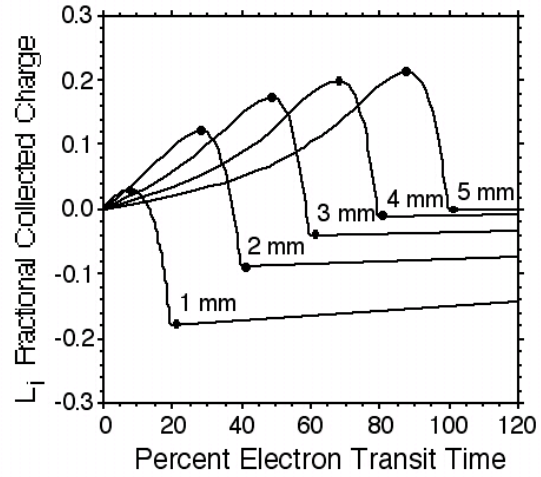

Fig. 5: Fig. 2 case: L_i signals vs interact-ion depth z for x = 0.85w. Transit time in ns.

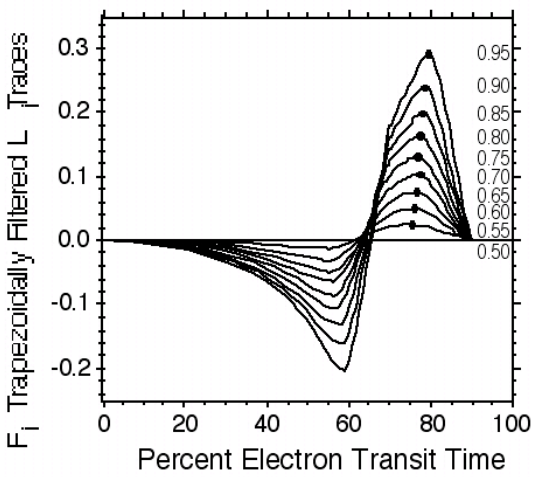

Fig. 6: 25ns/25ns trapezoidally filtered L_i signals F_i.

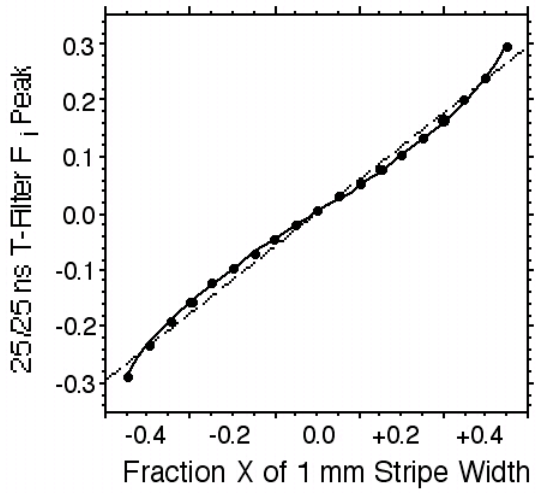

Fig. 7: Peak F_i values as a function of x, showing deviations from linearity.

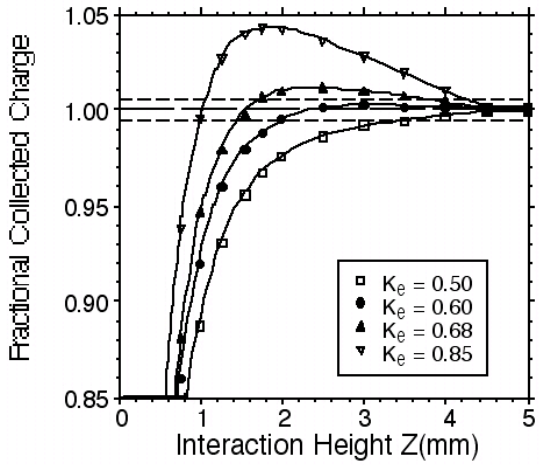

Fig. 8: Collected Energy signal E_i vs interaction depth z and parameter K_e.

DETERMINING PHOTON ENERGY

While Eqn 2a for E_i provides a first order correction for induced hole charge effects, it cannot be expected to be perfect because the geometries that the three pixels i-1, i, and i+1 present to the charge are different. These effects become particularly significant as z approaches w. To a certain extent, however, they may be balanced by an appropriate choice of the value K_e. Figure 8 shows values of Q_i, measured just after the electron collection is complete, versus z for several K_e values for a case with 1 mm stripe widths. The value 0.60 produces accuracies to 0.5% over the upper 2.5 mm of the detector. The value 0.68 produces accuracies to 1.5% over the upper 3.5 mm. The failure of the method for z below 1 mm is also apparent. In principle, timing information from T_i and S_i could be used to reject signals from photons absorbing at small z values.

The results presented in Figure 8 were computed assuming no carrier losses due to either electron or hole trapping. CZT, however, has significant values for both, with typical lifetimes in the few microsecond range. Trapped charges affect the signals of Eqn. 2 both by reducing "contrast" since they continue to induce charges on both i and neighbor pixels after "collection" is complete, and they reduce signal size since fewer carriers are "collected". Figure 9 shows how Fig. 8 is modified when literature values of hole and electron lifetimes are taken into account. The range of 0.5% performance is reduced to 2 mm and of 1.5% performance to 3 mm.

As shown in Figure 10, the situation becomes even more severe for thicker detectors. In Fig. 10, a 1 cm thick piece of CZT with 1 mm stripes has 2000 V applied. The slope of the curves at large z are due to electron trapping, since the maximum electron transit time is about 0.5 μs. With a K_e value of about 0.10, it is possible to get about 5% resolution over the upper 8 mm of the detector, but difficult to get significantly better resolution over any volume.

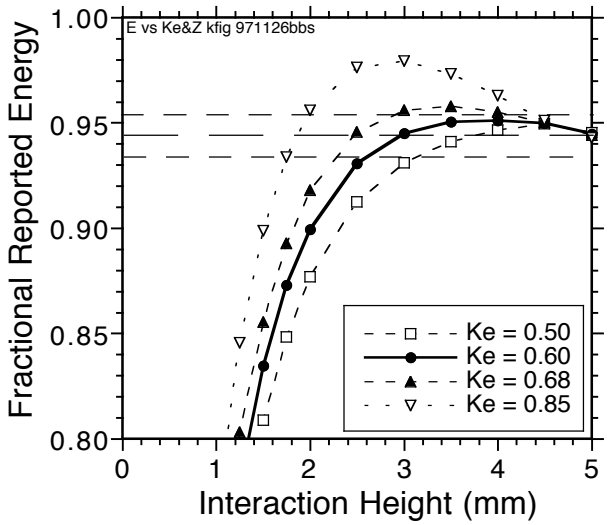

Fig. 9: Fig. 8 repeated with both hole and electron trapping.

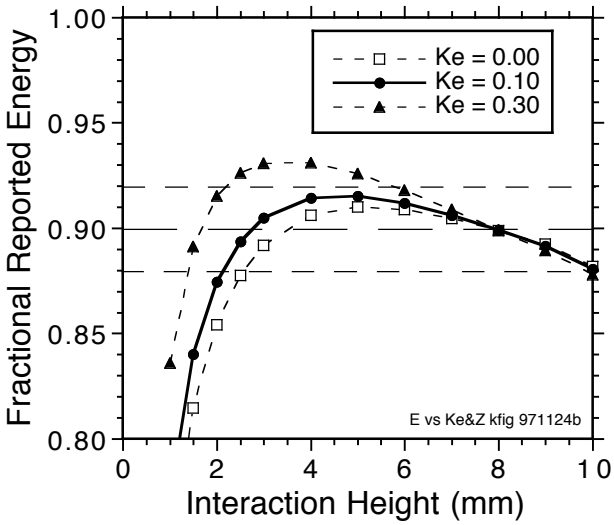

Fig. 10: Collected Energy signal E_i vs z and K_e in a 1 cm thick CZT detector with 1 mm stripes and 2000 V applied potential.

CONCLUSIONS

We have presented an approach to obtaining sub-pixel spatial resolution in thick detectors with stripe electrodes, although the same principles also apply to pixel electrodes. With 1 mm stripes, spatial resolutions in the 50 to 100 μm range are projected. Good energy resolutions can also be obtained in detectors up to 5 mm thick, but poor electron lifetimes preclude "spectroscopy grade" performance in thicker samples. Since this conclusion will also pertain to other induced charge approaches, it is clear that a high priority should be given to improving electron lifetimes in CZT if good energy resolution is to be obtained from thicker detectors.

ACKNOWLEDGMENTS

Part of this work was supported by the National Cancer Institute, National Institutes of Health through SBIR Grant 1 R43 CA75844-01.

REFERENCES

(See also: U.S. Patent 6,169,287 to William K. Warburton, January 2, 2001, "X-ray Detector Apparatus for Obtaining Spatial, Energy and/or Timing Information Using Signals From Neighboring Electrodes in an Electrode Array".)

1. W. K. Warburton in "Fifth Scientific Symposium on Room-Temperature Semi-Conductor X-ray, Gamma-ray, and Neutron Detectors, (11-12 March 1997, Sandia National Laboratory, Livermore, CA), Ed. R. B. James.
2. HB Barber, SPIE Vol. 2859, p.26-28 (1996).
3. LA Hamel, JR Macri, CM Stahle, J. Odom, F. Birsa, P. Shu & FP Doty, IEEE Trans. Nucl. Sci. **43**, p. 1422-1426 (1996).
4. DG Marks, HB Barber, EL Dereniak, JD Eskin, KJ Matherson, JM Woolfenden, ET Young, FL Augustine, WJ Hamilton, JE Venzon, BA Apotovsky & FP Doty, IEEE Trans. Nucl. Sci. **43**, p. 1253-1259 (1996).
5. JD Eskin, HH Barrett, HB Barber & JM Woolfenden, IEEE 1995 Nuclear Science Symposium and Medical Imaging Conference Record, P.A. Moonier Ed., p. 544-548 (1995).

PUBLISHED VERSION

The final version of this paper was published in "Semiconductors for Room-Temperature Radiation Detector Applications II", Eds. R.B. James et al., Mat. Res. Symp. Proc. **487**, 531-535 (1988).